

---

## HIGH-PERFORMANCE POSITION CONTROL OF SWITCHED RELUCTANCE MOTOR DRIVES BY USING FUZZY LOGIC

M. Divakar and V. V. Narasimha Murthy

M-tech Student Scholar , Department of Electrical and Electronics Engineering,  
University College Of Engineering Kakinada, JNTUK; A.P, India.  
Associate Professor , Department of Electrical & Electronics Engineering,  
University College Of Engineering Kakinada, JNTUK;A.P,India.

---

### Abstract

*The SRM drive operates over the entire speed range and provides low torque ripple with smooth transition between the control operations. The low torque ripple is achieved by controlling the firing angles through simple formulas so as to minimize the pulsations of the total current in the commutation region. The smooth transition is attained since the conditions that determine the firing angles of one operating mode are derived from the conditions of the other operating mode. This is important since the position precision is highly influenced from the motor torque ripple. The problem of high-precision position control in switched reluctance motor (SRM) drives is investigated in this paper. Advanced proportional–integral and Fuzzy proportional–differential controllers for speed and position controls, respectively are adopted. A gain-scheduling technique is adopted in the speed controller design for providing high dynamic performance and precise position control. The SRM drive is modeled in Simulink environment and several simulation results are presented to validate the feasibility of the proposed control scheme.*

---

### KEY WORDS:

Current control, PI control, Fuzzy PD control, switched reluctance motor (SRM) drives, torque control, variable-speed drives.

### I.INTRODUCTION

The last years and several papers have been published introducing the Switched Reluctance Machines (SRMs) as a strong-candidate. The SRM can operate as a motor as well as a generator by adjusting the firing angles . At low speeds, the torque is limited by the current which is controlled either by voltage-PWM or current regulation (PWM mode). At high speeds, the available voltage is insufficient to regulate the current and the torque is controlled by the duration of the current pulses (single pulse mode). Although the SRMs have some very attractive characteristics, their acceptance by the industry for variable speed applications is very slow. The torque ripple remains a serious problem for servo drive applications. Significant effort has been made over the past decades to overcome this problem by improving the magnetic design of the machine or by introducing sophisticated control techniques.

In recent years, SRMs have attracted renewed interest due to the tendency to shift from the complex design and precise manufacturing to the highly effective and more sophisticated control. The improvement in control algorithms and techniques can extract good performance from a simple SRM drive and result in increasing the penetration of the SRM drives in highly demanding applications [4]. This can give new trends in motor drive applications and open new horizons in the existing field of advanced motor drive engineering.

The present technical literature seldom targets to developments the SRM for high-precision position control applications. In [4]–[8], the problem of rotor position sensing has been investigated, and several sensorless control techniques for speed control operation have been proposed. A micro step

control strategy realized with a fuzzy-logic-based controller was proposed in [9]. However, the position precision is limited to a predefined step angle. A position control system was presented in [10], but only response characteristics of the position controller in slow ramp-shape command position were examined. Basic four-quadrant sensorless configurations for SRM drives have been described in [11] and [12].

The development of linear motion actuator systems for position control applications was presented in [12] and [14]. A self-tuning regulator for obtaining high-precision position control of a linear SRM drive was proposed in [15]. A position control system with a 2-D planar SRM was described in [3]. The control of SRMs requires proper synchronization of rotor position with the pulses of phase currents. Multiphase switching is mandatory for both minimizing the torque ripple and delivering high and quickly responsive torque performance. The large stroke angle is an obstacle if high-precision position control is desired. However, a proper control strategy that is based on adaptation of the controller parameters could compensate this drawback. The proportional–integral–differential (PID) control offers the simplest and efficient solution that is needed for an automatic control system with SRM. The designing and tuning of a PID controller are rather intuitive, but the introduction of some advanced control techniques could result to an SRM control system that satisfies the control objectives of stability with short and smooth transient response.

A new four-quadrant multimode SRM control scheme is proposed that provides low torque ripple and smooth transition between the control operations with the average torque control method. The controller on-line determines the optimal turn-on and turn-off angles for all operating modes through simple formulas that could serve as optimal conditions. The suggested controller is simple and can be easily implemented since the knowledge of the machine magnetization curves is not required. Several simulation results from a SRM drive model developed in Simulink environment are presented to validate the theoretical considerations.

## II. SRM OPERATING PRINCIPLES

The SRM has a highly nonlinear characteristic due to its nonlinear flux behaviour. The voltage equation for each phase  $j$  is given by

$$u_j = R_j i_j + (d\lambda_j(i, \theta))/dt \text{ -----(a)}$$

and the rate of change of the flux linkage, at constant speed, is

$$\frac{d\lambda_i}{dt} = \frac{\partial \lambda_i}{\partial i} \frac{di}{dt} + \frac{\partial \lambda_i}{\partial \theta} \omega_r = L_j(i, \theta) \frac{di}{dt} + e_j \text{---(b)}$$

where  $L_j(i, \theta) = \lambda_j / i$  is the incremental inductance (slope of the magnetization curve at the position  $\theta$ ),  $e_i$  is the back electromotive force (EMF),  $u_j$  is the applied voltage,  $i_j$  is the phase current,  $R_i$  is the winding resistance per phase,  $\lambda_j$  is the phase flux linkage, and  $\theta$  is the mechanical angle [a].

The instantaneous electromagnetic torque produced by each phase is given from the partial derivative of the phase co-energy and is defined by

$$T_j(i, \theta) = \frac{\partial W_{ej}(i, \theta)}{\partial \theta} \text{ where } i \text{ is constant ---(c)}$$

Where

$$W_{ci} = \int_0^i \lambda_j(e, \theta) \text{ where } \theta \text{ is constant ----(d)}$$

The total instantaneous electromagnetic torque is given by the sum of the individual phase torques

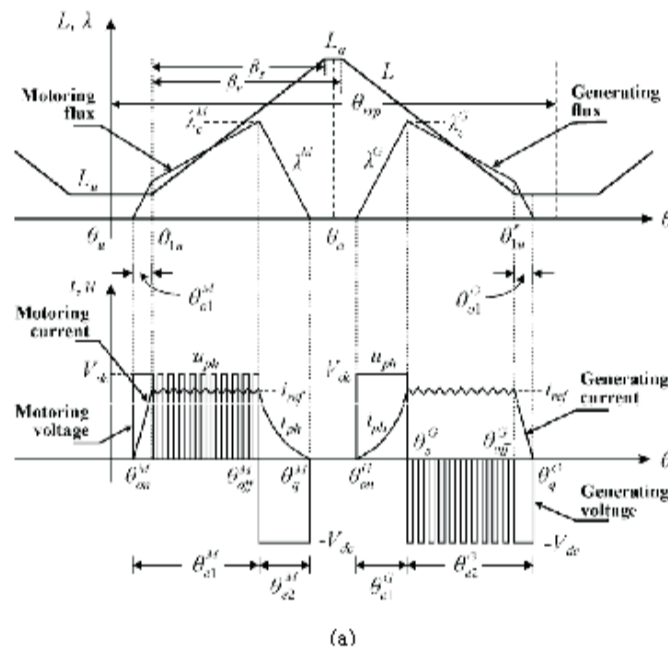
$$T_e = \sum_{j=1}^m T_j(i, \theta) \text{ ----- (e)}$$

where  $m$  is the number of SRM phases [e].

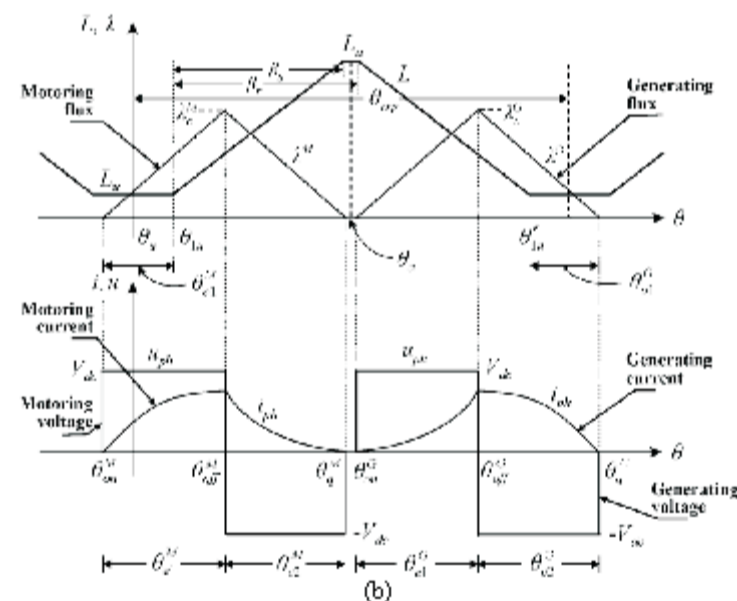
The electromagnetic torque of an SRM can be described by the nonlinear torque–current–angle (T- i- ) data. The magnetic nonlinearities of the machine can be taken into account through the appropriate modeling of the nonlinear flux–current–angle ( - i- ) characteristics. The machine model consists of lookup tables, with the flux linkage ( , ) and the static torque  $T_e(i , )$  expressed as functions of current level  $i$  and rotor position .

**III. DEFINING THE TURN-ON AND TURN-OFF ANGLE CONDITIONS FOR SMOOTH TORQUE CONTROL**

The torque pulsations in a SRM are due to the discrete nature of torque production mechanism. The SRM stator phases are independently controlled and the total torque is the sum of the torques generated by each of the phases. Torque pulsations are stronger at the commutation intervals because the two adjacent phases produce additive torques. Therefore, it is possible to minimize the torque ripple by controlling the turn-on and turn-off angles, so that the sum of all phase currents provides a smooth total current waveform.



(a)



(b)

Fig. 1. Typical SRM drive waveforms in motoring and generating operation: (a) PWM soft chopping current control and (b) single pulse control.

### A. Motoring Operation

In PWM current-controlled motoring operation, the turn-on angle is selected so that the phase current acquires its reference value  $i_{ref}$  on the angle  $\theta_{1u}^M$  ( $\theta_s^M = \theta_{1u}^M$ ) at which the stator and rotor poles start to overlap and the inductance start rising [8]. This allows the phase current to increase up to its reference value while the inductance is still low and there is no back-emf that would oppose the current increase. If winding resistance and fringing effect are ignored, the turn-on angle is determined by

$$\theta_{on}^M = \theta_{1u}^M - \frac{L_u i_{ref} \omega_r}{V_{dc}} \quad (1)$$

Fig. 2(a) illustrates the flux-linkage and current profiles of two neighboring phases in PWM motoring operation. For providing smooth current transfer between adjacent phases, the firing angles are controlled so that the  $\theta_{off}^M$  interval is equal to the half of the de-fluxing period  $\theta_{e2}^M$

$$\theta_{off}^M = \frac{\theta_{e2}^M}{2} \quad (2)$$

Substituting (2) in (1), the turn-on angle condition becomes

$$\theta_{on}^M = \theta_{1u}^M - \frac{\theta_{e2}^M}{2} \quad (3)$$

Since the peak flux-linkage at the turn-off angle is given by

$$\lambda_c^M = \frac{V_{dc} \theta_{e2}^M}{\omega_r} \quad (4)$$

and the flux-linkage at the angle  $\theta_{1u}^M$  is

$$\lambda_d^M = \frac{V_{dc} \theta_{o1}^M}{\omega_r} \quad (5)$$

it is obtained

$$\frac{\lambda_c^M}{\lambda_d^M} = \frac{\theta_{e2}^M}{\theta_{o1}^M} \quad (6)$$

From (2) and (6) it is concluded

$$\lambda_d^M = \frac{\lambda_c^M}{2} \quad (7)$$

Therefore, the turn-on angle of the incoming phase 2 should coincide with the turn-off angle of the outgoing phase 1 and consequently, the dwell period is equal to the stroke angle ( $\theta_{e1}^M = \theta_{sk}^M$ ). Thus, the turn-off angle for smooth torque PWM motoring operation is determined by

$$\theta_{off}^M = \theta_{on}^M + \theta_{sk}^M \quad (8)$$

At high speeds, the SRM turns to single pulse mode because the motor back-emf is larger than the dc-link voltage and there is no control over the phase current. Then, the torque is controlled by

varying the firing angles of a single current pulse, Fig. 2(b).

In order to provide smooth current transfer between adjacent phases, condition 2) holds for single pulse control and turn-on angle is determined by (3), as for the PWM control. Taking into account that in single-pulse mode the dwell period is almost equal to the de-fluxing period)

( $\theta_{e1}^M = \theta_{e2}^M$ ), the turnoff angle is obtained by

$$\theta_{off}^M = \theta_{on}^M + \theta_{e2}^M \quad (9)$$

Note that, due to (2), condition (7) is also valid for single pulse mode. However, the flux-linkage in the intersection angle  $\theta_i^M$  is greater than the half of the peak flux linkage,  $\lambda_i^M > \lambda_c^M/2$  and therefore higher torque ripple is expected compared to PWM mode at which  $\lambda_i^M = \lambda_d^M = \lambda_c^M/2$

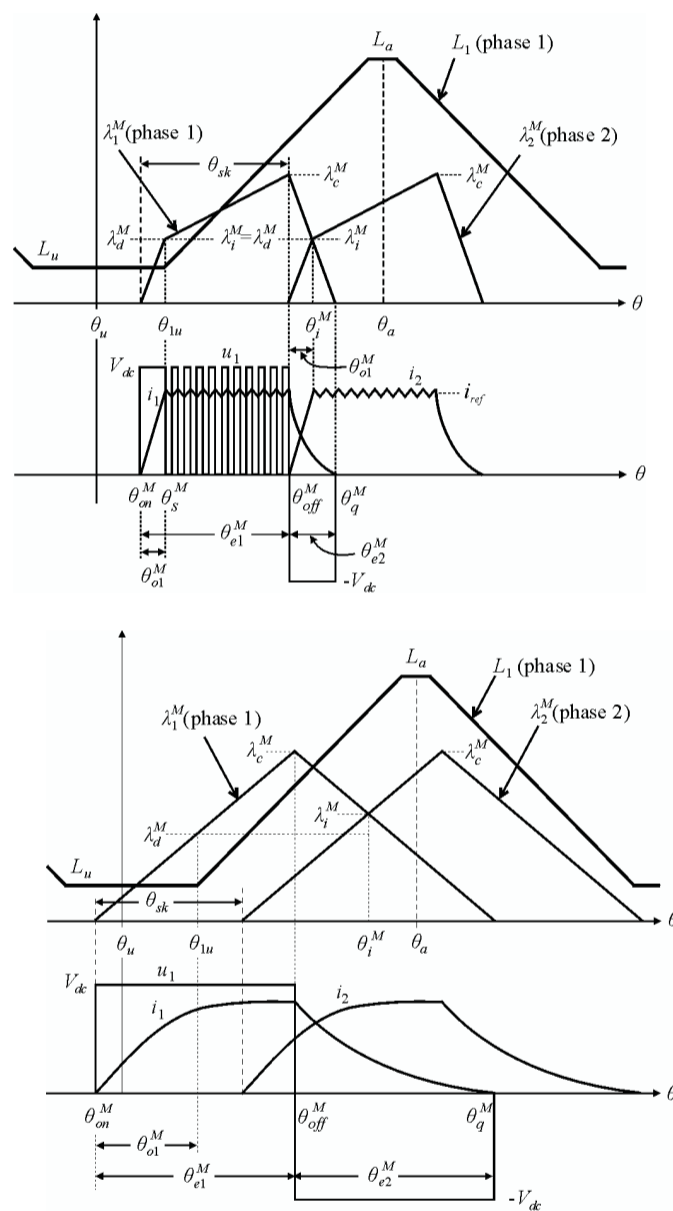


**Fig. 2. Typical SRM waveforms in motoring operation considering the overlapping flux-linkage and current profiles of two neighboring phases: (a) PWM soft chopping control and (b) single pulse control.**

### B. Generating Operation

Fig. 3(a) illustrates the flux-linkage and current waveforms of two neighboring phases in PWM

generating operation. During the  $\theta_{01}^G$  interval, the stored field energy is returned to the dc-link and if it exploits the unaligned region, the stored field energy is released without extracting mechanical energy from the prime mover. Therefore, the turn-off angle is selected at the rotor position that stator and rotor pole corners complete overlap

$$\theta_{off}^G = \theta_{1u}^G \quad (10)$$

As in motoring operation, torque ripple is minimized by providing smooth current transfer between adjacent phases. Therefore, the  $\theta_{01}^G$  interval should be equal to the half of the dwell period  $\theta_{e1}^G$ .

$$\theta_{01}^G = \frac{\theta_{e1}^G}{2} \quad (11)$$

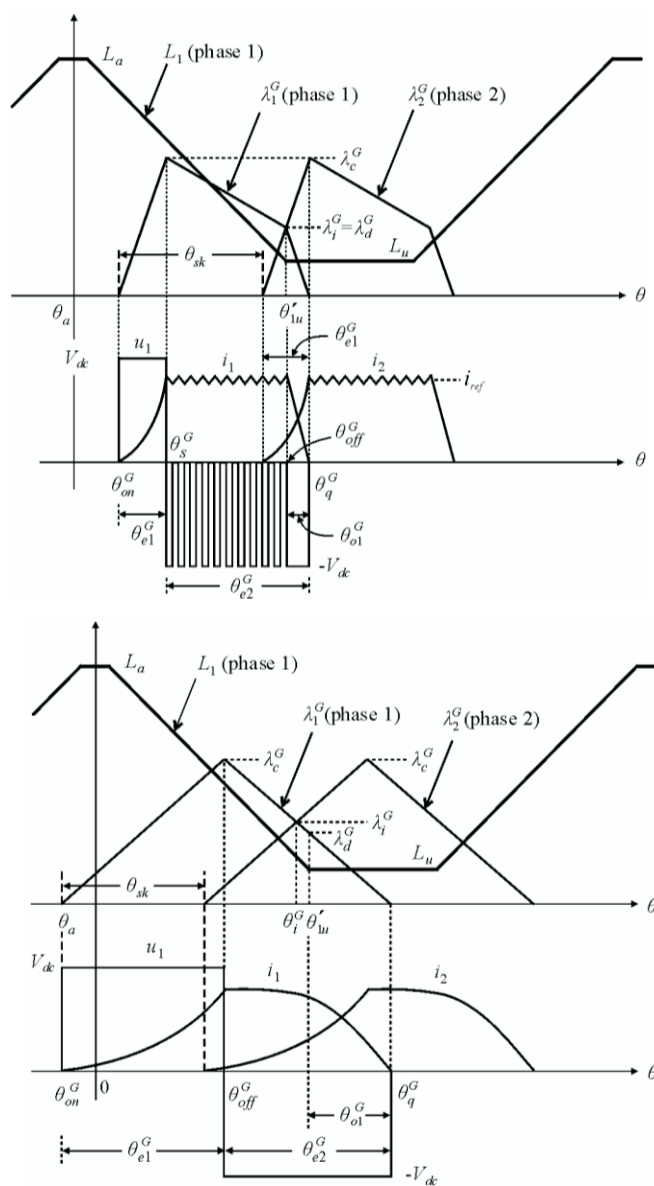


Fig. 3. Typical SRM waveforms in generating operation considering the overlapping flux-linkage and current profiles of two neighboring phases: (a) PWM soft chopping control and (b) single pulse control

From Fig. 3(a) and using (10) and (11), the turn-on angle condition for providing smooth torque in PWM generating operation is defined by

$$\theta_{sk}^G = \theta_{1u}^G + \left( \theta_{sk} - \frac{\theta_{e1}^G}{2} \right) \quad (18)$$

Using (12), the  $\theta_s^G$  angle at which current reaches its reference value  $i_{ref}$  is given by

$$\theta_s^G = \theta_{on}^G + \theta_{e1}^G = \theta_{e1}^G - \left( \theta_{sk} - \frac{\theta_{e1}^G}{2} \right) \quad (19)$$

From (10) and (11) it is concluded that

$$\lambda_d^G = \frac{\lambda_c^G}{2} \quad (20)$$

$$\lambda_c^G = \frac{V_{dc} \theta_{e1}^G}{\omega_r} \quad (21)$$

$$\lambda_d^G = \frac{V_{dc} \theta_{o1}^G}{\omega_r} \quad (22)$$

As in motoring operation, condition (11) of PWM control holds for single pulse, too. From Fig. 3(b) and taking into account that  $\theta_{e1}^G = \theta_{e2}^G$ , it is concluded that the turn-on and turn-off angle conditions, respectively, for single pulse generating operation are given by

$$\theta_{on}^G = \theta_{1u}^G - \frac{3}{2} \theta_{e1}^G \quad (23)$$

$$\theta_{off}^G = \theta_{on}^G + \theta_{e1}^G = \theta_{1u}^G - \frac{\theta_{e1}^G}{2} \quad (24)$$

As in motoring operation, the flux-linkage in the intersection angle  $\theta_i^G$  is greater than the half of the peak flux linkage,  $\lambda_i^G > \lambda_c^G/2$  and therefore, higher torque ripple is expected compared to PWM mode at which  $\lambda_i^G = \lambda_d^G = \lambda_c^G/2$ .

#### IV. DESIGN AND IMPLEMENTATION OF THE CONTROL SYSTEM

The feedback system with the speed and position controllers is shown in Fig. 4. The transfer function  $G_p(s)$  represents the SRM and the power converter. In the speed PI controller, an anti windup protection is used in order to avoid low-frequency oscillations that may lead to instability. This is realized by applying inner negative feedback to the integral action of the controller.

The Simu link diagram of the SRM drive that is used in simulations is shown in Fig. 5. The same controller model, in combination with the I/O interface blocks provided by the board supporting software, was used for programming the DSP controller board. Fig. 6(a) and (b) shows the Simu link diagrams of the advanced speed and fuzzy position controllers of the SRM drive, respectively. The block "Firing angles" determines

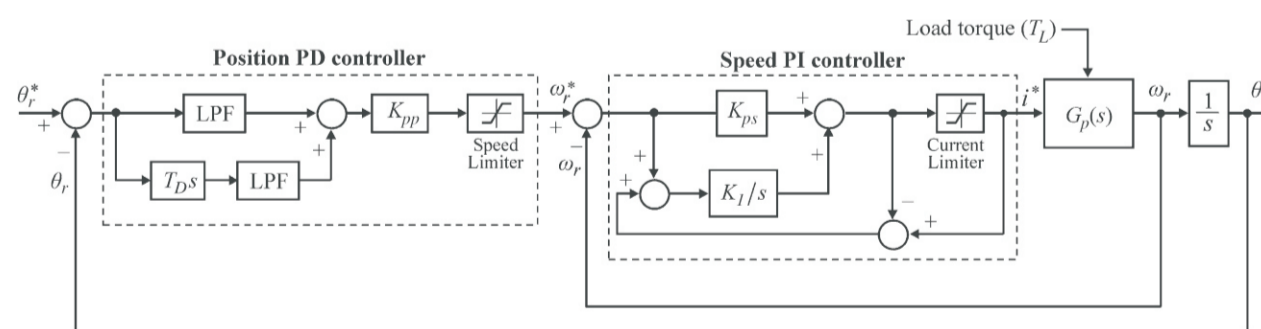
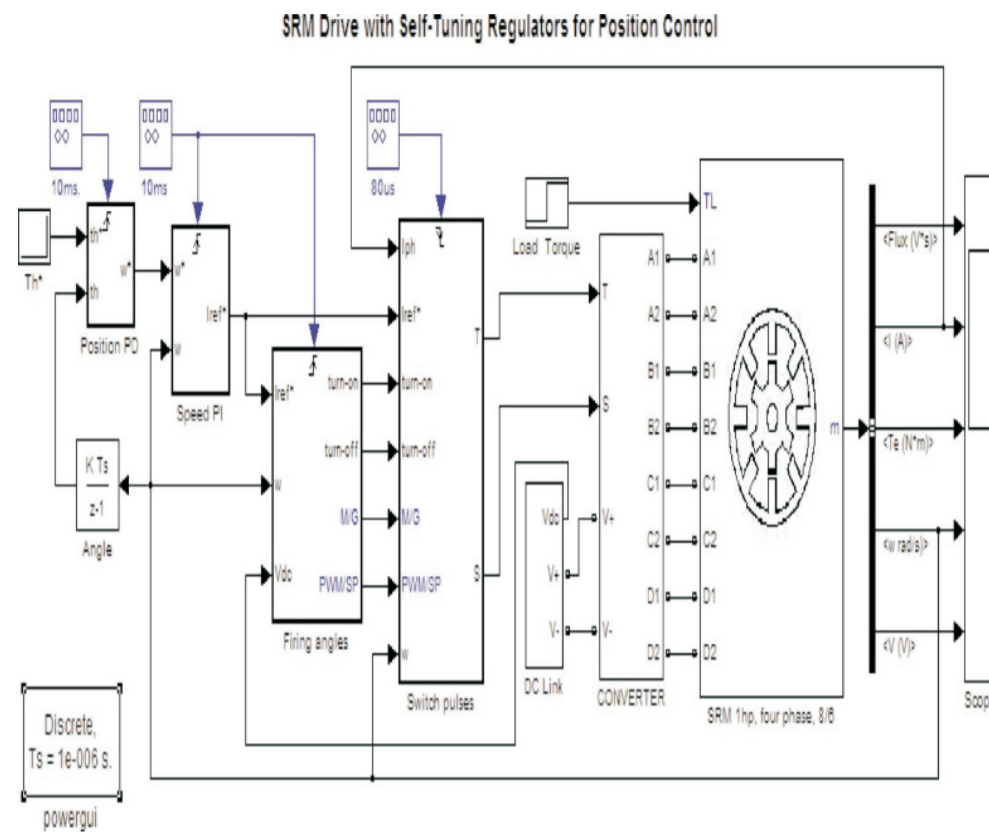


Fig. 4. Model configuration of the advanced speed and position controllers.



**Fig. 5. Simulink diagram of the SRM drive with advanced speed PI and position PD controllers.**

the command turn-on and turn-off angles, i.e.,  $\theta^*_{on}$  and  $\theta^*_{off}$ ] respectively, through the conditions presented in Section III. The block “Switch pulses” generates the control pulses for the SRM power converter switches. In the low-speed region, the phase current is regulated by a hysteresis-band PWM control technique.

The block “Speed PI” determines the reference phase current  $i^*$  through the speed error  $(\omega^* - \omega)$ . The gains  $K_I$  and  $K_p$  of the PI controller are online adapted. The lookup table  $T(i, \theta)$  was determined by means of offline experiments of the SRM drive.

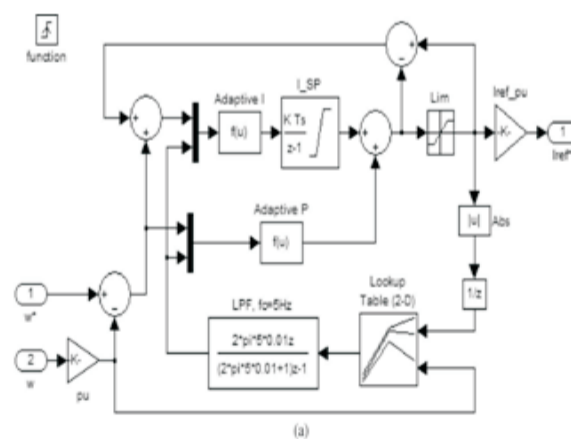


**Fig6.a.Speed PI Control**



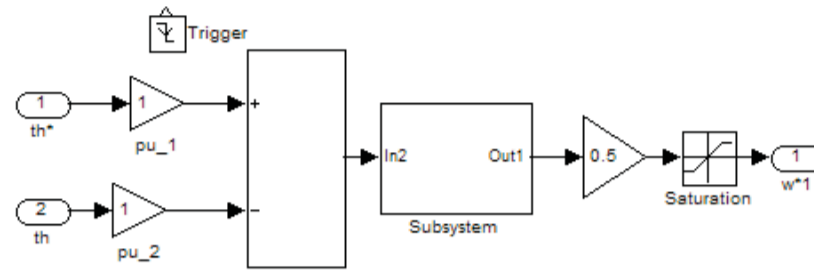


Fig6.b. Fuzzy PD control

V.SIMULATION RESULTS

A four-phase 1-hp 8/6 SRM drive was used to validate the developed position control system. The parameters of the motor are reported in Table I. The controller board DS-1104 of dSPACE was used for the implementation of the experimental system. Fig. 7 shows the variation of torque ripple factor as defined by

$$K_{rip} = \frac{t_{max} - t_{min}}{T_{avg}} \text{ ----- (2)}$$

where  $T_{min}$  and  $T_{max}$  are the minimum and maximum instantaneous torques, respectively, for each given SRM speed, while  $T_{avg}$  is the average torque. Fig. 7(a) corresponds to a PWM operation, while Fig. 7(b) corresponds to a single-pulse peration. All points noted by asterisk correspond to operating points obtained with the firing angle conditions of Section III. It can be seen that, in these points, minimum torque ripple is achieved.

Output power 1-hp at 4,000 rpm (motoring operation)

Inertia 0.0004 Kg·m<sup>2</sup>

$$m = 4$$

$$\beta_s = 23^0$$

$$N_s/N_r = 8/6$$

$$\beta_r = 23.4^0$$

$$\theta_{rrp} = 2\pi/N_r = 60^0$$

$$R_{ph} = 1.3 \Omega$$

$$L_a = 52.7 \text{ mH}$$

$$L_u = 9.1 \text{ mH}$$

TABLE I  
FOUR-PHASE 1-hp 8/6 SRM

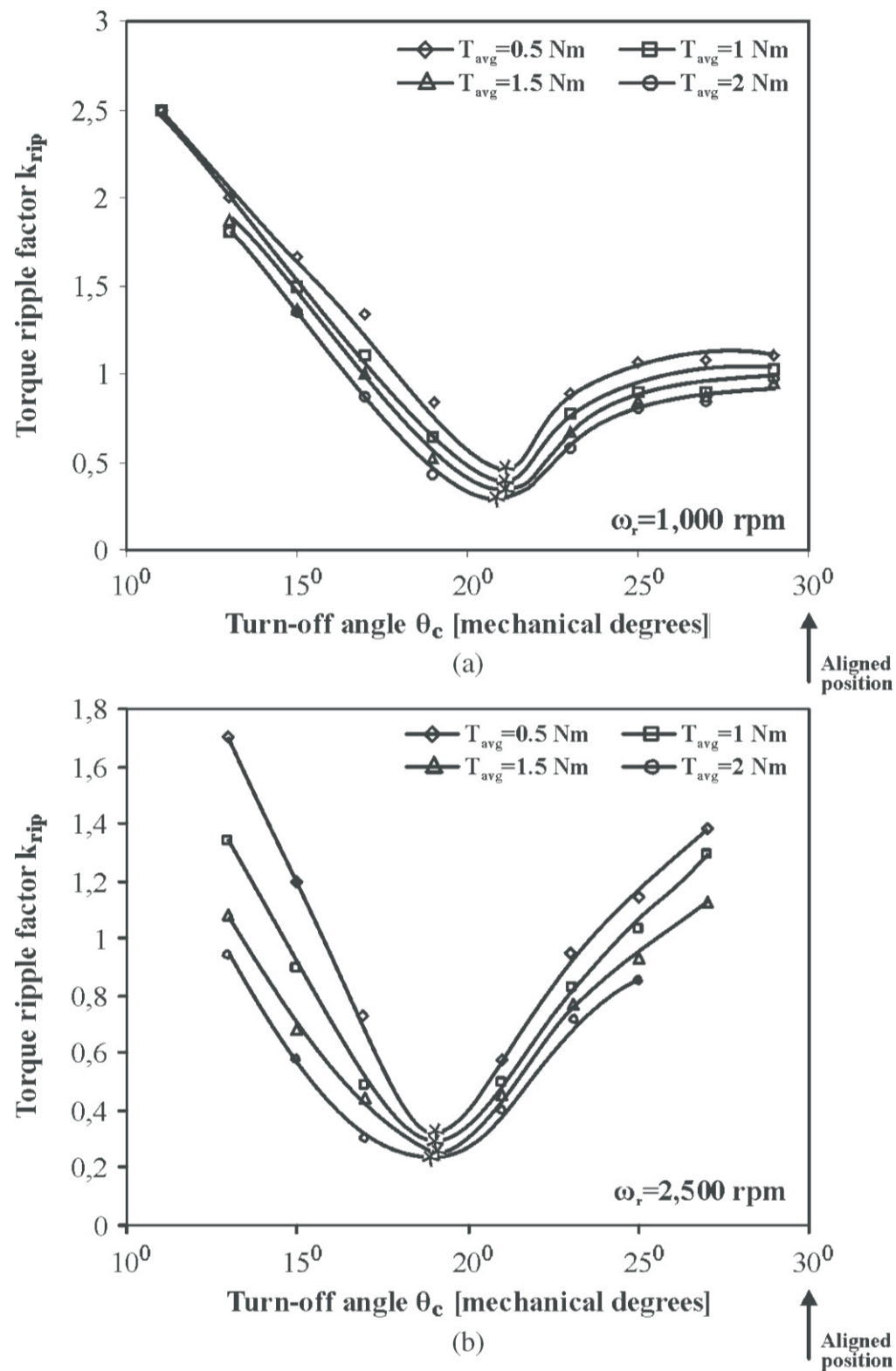
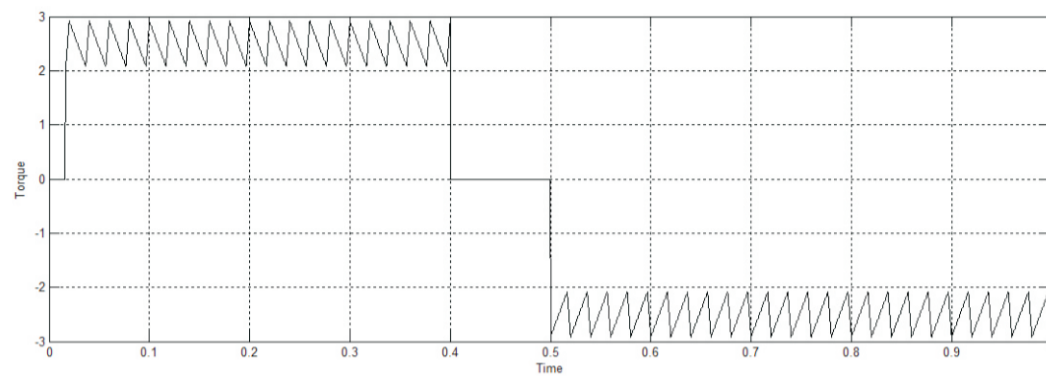
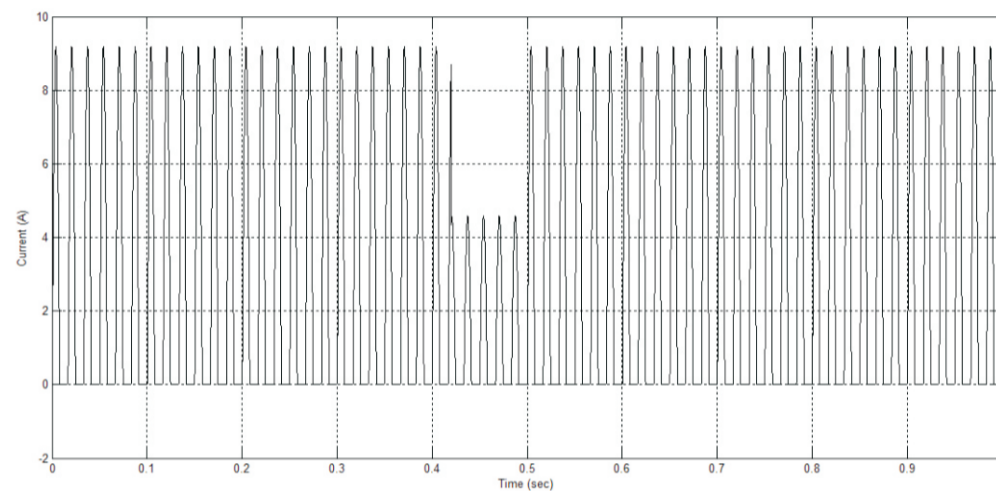


Fig. 7. Variation of torque ripple factor, as defined in (29), for various speeds and load torque values, in a four-phase 1-hp 8/6 SRMdrive. (a) PWMoperation. (b) Single-pulse operation.



**Fig8. Torque graph when it changes from Motoring mode to Breaking mode**



**Figure9. Current graph when it turns from motoring to braking operation**

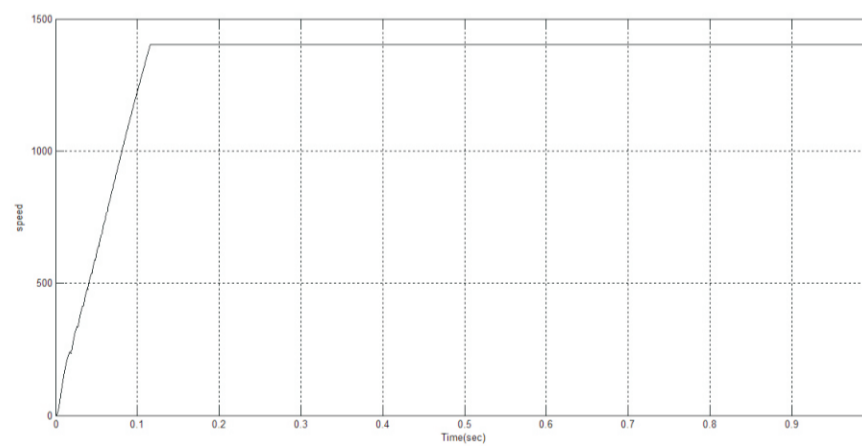


**Figure 10. Speed graph**

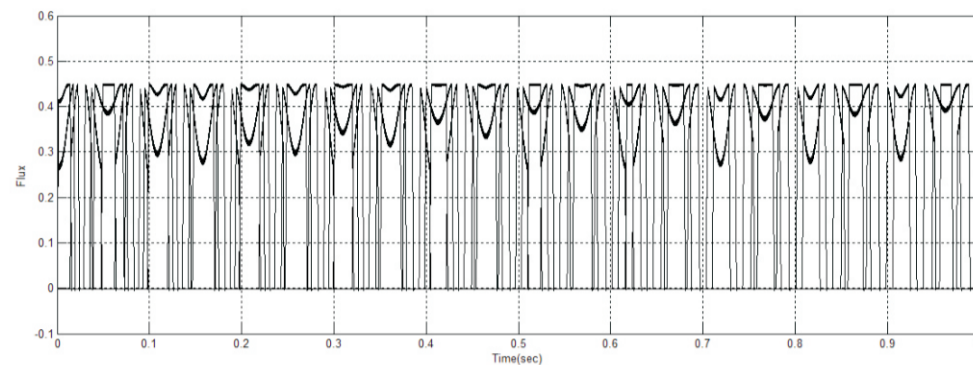


**Figure11. Flux graph**

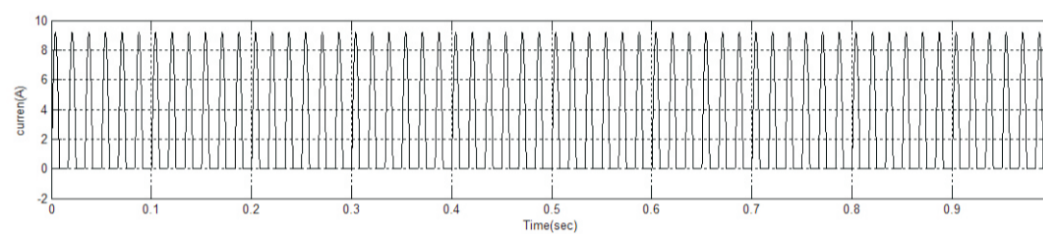


**Figure 12. Current in motoring operation**

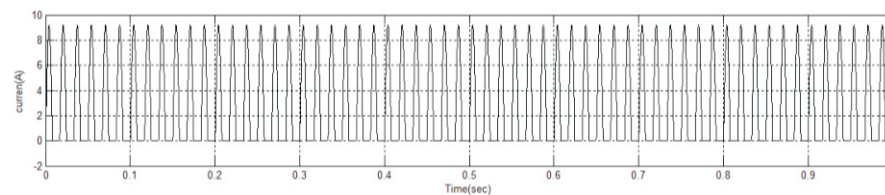


**Figure 13. Current in braking operation**

## VI.CONCLUSION

The four-quadrant control scheme is based on the average torque control method, and it is capable for maintaining the torque ripple at an acceptable level over a wide speed range. Advanced PI control and Fuzzy PD control have been presented in this paper. The parameters of the speed PI controller are online adjusted according to the load torque and rotor speed. A smooth transition between PWM and single pulse modes is provided, since the firing angle conditions are continuous functions at the points where the SRM operation mode is changed. The four-quadrant control scheme is based on the average torque control method, and it is capable for maintaining the torque ripple at an acceptable level over a wide speed range. Thus, it provides quick response and high-precision position control of the SRM drive. The proposed controller is easily implemented and does not require the knowledge of the SRM magnetization curves. Several simulation results are presented to validate the feasibility of the proposed control scheme.

## REFERENCES

- [1]. Christos Mademlis, Member, IEEE, and Iordanis Kioskeridis, Member, IEEE "Gain-Scheduling Regulator for High-Performance Position Control of Switched Reluctance Motor Drives".
- [2] C. Mademlis and I. Kioskeridis, "Four-quadrant smooth torque controlled Switched Reluctance Machine drives," in Proc.

- [3] J. Pan, N. C. Cheung, and J. Yang, "High-precision position control of a novel planar switched reluctance motor," *IEEE Trans. Ind. Electron.*, vol. 52, no. 6, pp. 1644–1652, Dec. 2005.
- [4] I. Husain and M. Ehsani, "Error analysis in indirect rotor position sensing of switched reluctance motors," *IEEE Trans. Ind. Electron.*, vol. 41, no. 3, pp. 301–307, Jun. 1994.
- [5] I. W. Yang and Y. S. Kim, "Rotor speed and position sensorless control of a switched reluctance motor using the binary observer," *Proc. Inst. Elect. Eng.—Electr. Power Appl.*, vol. 147, no. 3, pp. 220–226, May 2000.
- [6] M. Ehsani and B. Fahimi, "Elimination of position sensorless in switched reluctance motor drives: State of the art and future trends," *IEEE Trans. Ind. Electron.*, vol. 49, no. 1, pp. 40–47, Feb. 2002.
- [7] A. D. Cheok and Z. Wang, "Fuzzy logic rotor position estimation based switched reluctance motor DSP drive with accuracy enhancement," *IEEE Trans. Power Electron.*, vol. 20, no. 4, pp. 908–921, Jul. 2005.
- [8] M. Krishnamurthy, C. S. Edrington, and B. Fahimi, "Prediction of rotor position at standstill and rotating shaft conditions in switched reluctance machines," *IEEE Trans. Power Electron.*, vol. 21, no. 1, pp. 225–233, Jan. 2006. EE PESC, Rhodes, Greece, Jun. 2008, pp. 1216–1222.
- [9] G. Song, H. Sun, L. Huang, and J. Chu, "Micro-step position control of switched reluctance motors," in *Proc. Conf. PEDS*, Nov. 2003, vol. 2, pp. 944–947.
- [10] M. H. Kim, W. S. Baik, D. H. Kim, and K. H. Choi, "A high performance position control system of switched reluctance motor," in *Proc. PCC*, Nagoya, Japan, Apr. 2007, pp. 249–252.
- [11] S. Hossain, I. Husain, H. Klode, A. Omekanda, and S. Gopalakrishnan, "Four quadrant and zero speed sensorless control of a switched reluctance motor," *IEEE Trans. Ind. Appl.*, vol. 39, no. 5, pp. 1343–1349, Sep./Oct. 2003.
- [12] B. Fahimi, A. Emadi, and R. B. Sepe, Jr., "Four-quadrant position sensorless control in SRM drives over the entire speed range," *IEEE Trans. Power Electron.*, vol. 20, no. 1, pp. 154–163, Jan. 2005.
- [13] W. C. Gan, N. C. Cheung, and L. Qiu, "Position control of linear switched reluctance motors for high-precision applications," *IEEE Trans. Ind.*
- [14] L. Yuan-Jiang, G. P. Widdowson, S. Y. Ho, G. W. Chuen, and P. Borsje, "Design and analysis of linear switched reluctance motor for high precision control," in *Proc. IEMDC*, May 2007, vol. 1, pp. 55–58.
- [15] S. W. Zhao, N. C. Cheung, W.-C. Gan, J. M. Yang, and J. F. Pan, "A self-tuning regulator for the high-precision control of a linear switched reluctance motor," *IEEE Trans. Ind. Electron.*, vol. 54, no. 5, pp. 2425–2434, Oct. 2007.
- [16] X. D. Xue, K. W. E. Cheng, and S. L. Ho, "A self-training numerical method to calculate the magnetic characteristics for switched reluctance motor drives," *IEEE Trans. Magn.*, vol. 40, no. 2, pp. 734–737, Mar. 2004.
- [71] K. J. Åström and B. Wittenmark, *Computer Controlled Systems*, 3rd ed. Englewood Cliffs, NJ: Prentice-Hall, 1996.
- [18] G. Orelind, L. Wozniak, J. Medanic, and T. Whittemore, "Optimal PID gain schedule for hydrogenerators—Design and applications," *IEEE Trans. Energy Convers.*, vol. 4, no. 3, pp. 300–307, Sep. 1989.
- [19] M. R. Mataušek, B. I. Jęftenia, D. M. Miljkoviæ, and M. Z. Bebiæ, "Gain scheduling control of DC motor drive with field weakening," *IEEE Trans. Ind. Electron.*, vol. 43, no. 1, pp. 153–162, Feb. 1996.
- [20] J. Talaq and F. Al-Basri, "Adaptive fuzzy gain scheduling for load frequency control," *IEEE Trans. Power Syst.*, vol. 14, no. 1, pp. 145–150, Feb. 1999.
- [21] W. K. Ho, S. K. Panda, K. W. Lim, and F. S. Huang, "Gain-scheduling control of the switched reluctance motor," *Control Eng. Pract.*, vol. 6, no. 2, pp. 181–189, Feb. 1998.
- [22] H. Hannoun, M. Hilairet, and C. Marchand, "Gain-scheduling PI current controller for a switched reluctance motor," in *Proc. Conf. ISIE*, Jun. 2007, pp. 1177–1182.
- [23] S. K. Panda, X. M. Zhu, and P. K. Dash, "Fuzzy gain scheduled PI speed controller for switched reluctance motor drive," in *Proc. IEEE IECON*, Nov. 1997, vol. 3, pp. 989–994.